

Electronic Supplementary Information

Ultra-Thin Film Composite Mixed Matrix Membranes incorporating Bio-inspired Iron(III)- dopamine Nanoparticles for CO₂ Separation

Jinguk Kim,^{a,b} Qiang Fu,^{ab} Joel M. P. Scofield,^{ab} Sandra E. Kentish^a and Greg G. Qiao^{ab}*

a Cooperative Research Centre for Greenhouse Gas Technology, Department of Chemical and Biomolecular Engineering, The University of Melbourne, VIC 3010, Australia

b Polymer Science Group, Department of Chemical and Biomolecular Engineering, The University of Melbourne, VIC 3010, Australia

*Corresponding author. Tel: +61 3 8344 8665; Fax: +61 3 8344 4153; E-mail:
gregghq@unimelb.edu.au (G. G. Qiao)

Table S1. Literature results in thin film composite (TFC) membranes for CO₂ separation over N₂.

Membrane material	Selective layer thickness [nm]	CO ₂ permeance [GPU]	α (CO ₂ /N ₂)	Ref.
PEO-PBT/PEG-DBE	500	518	50	[1]
Matrimid® 5218	330	20	23	[2]
PIM-1/ Matrimid® 5218	70	243	30	[3]
PDMS/PES/ Matrimid® 5218	110	60	39	[4]
PES/PI	270	12	30	[5]
PPO	430	100	21	[6]
PSf	2000	4.5	20	[7]
Pebax® 1657	500	157	64	[8]
Pebax® 1657/PEG	1000	65	80	[9]
Pebax® 1657/PDMS/PAN	300	482	42	[10]
Pebax® 2533/PSf	5000	61	30	[11]
BPVE-PFCB	10	1000	15	[12]
PES/DG	150	24	34	[13]
PI (PMDA-ODA)	100	750	15	[14]
PI (BPDA-PEO/ODA)	930	122	39	[15]
Ultem/PIM-1	74	34	30	[16]
6FDA-DAM-DABA	800	520	24	[17]

Table S2. Literature results in mixed matrix membranes (MMMs) for CO₂ separation over N₂.

Membrane material	Filler	Selective layer thickness [um]	CO ₂ permeance [GPU]	α (CO ₂ /N ₂)	Ref.
PDMS	PEG	-	14	67	[18]
PVA	FS, POS	24 – 32	29 - 42	-	[19]
PI	Silica	76	1.1	16	[20]
PI	ZIF	10	2.4	12	[21]
PAPE	GPTMS	80 – 150	0.83 – 1.6	89	[22]
Poly(RTIL)	Zeolite	580	1.1	34	[23]
PEI	ZIF	-	26	36	[24]
Pebax® 1657	ZIF	498	291	68	[25]
Pebax® 1657	MWCNT	20	1	59	[26]
Pebax® 1657	POSS	100	1.2	-	[27]
Matrimid® 5218	TiO ₂	80 – 120	0.09 – 0.13	11	[28]
Matrimid® 5218	MOF	35	0.58	39	[29]
Matrimid® 5218	CMS	30-60	0.28	33	[30]
PSf	MCM-41	24.5	0.84	27	[31]
PSf	SAPO-34	53-91	314	26	[32]
PES	13X, 4A	70-80	0.07, 0.15	43	[33]
PVAc	CuTPA (MOF)	58-91	0.044	36	[34]
PVAc	4A	70-90	0.03	100	[35]
BPPO	CNT	50-90	1.8	30	[36]

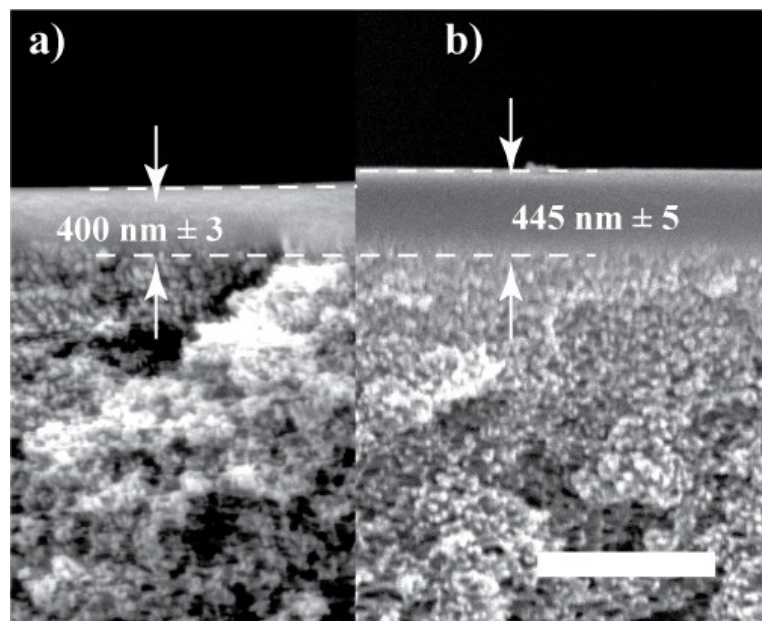
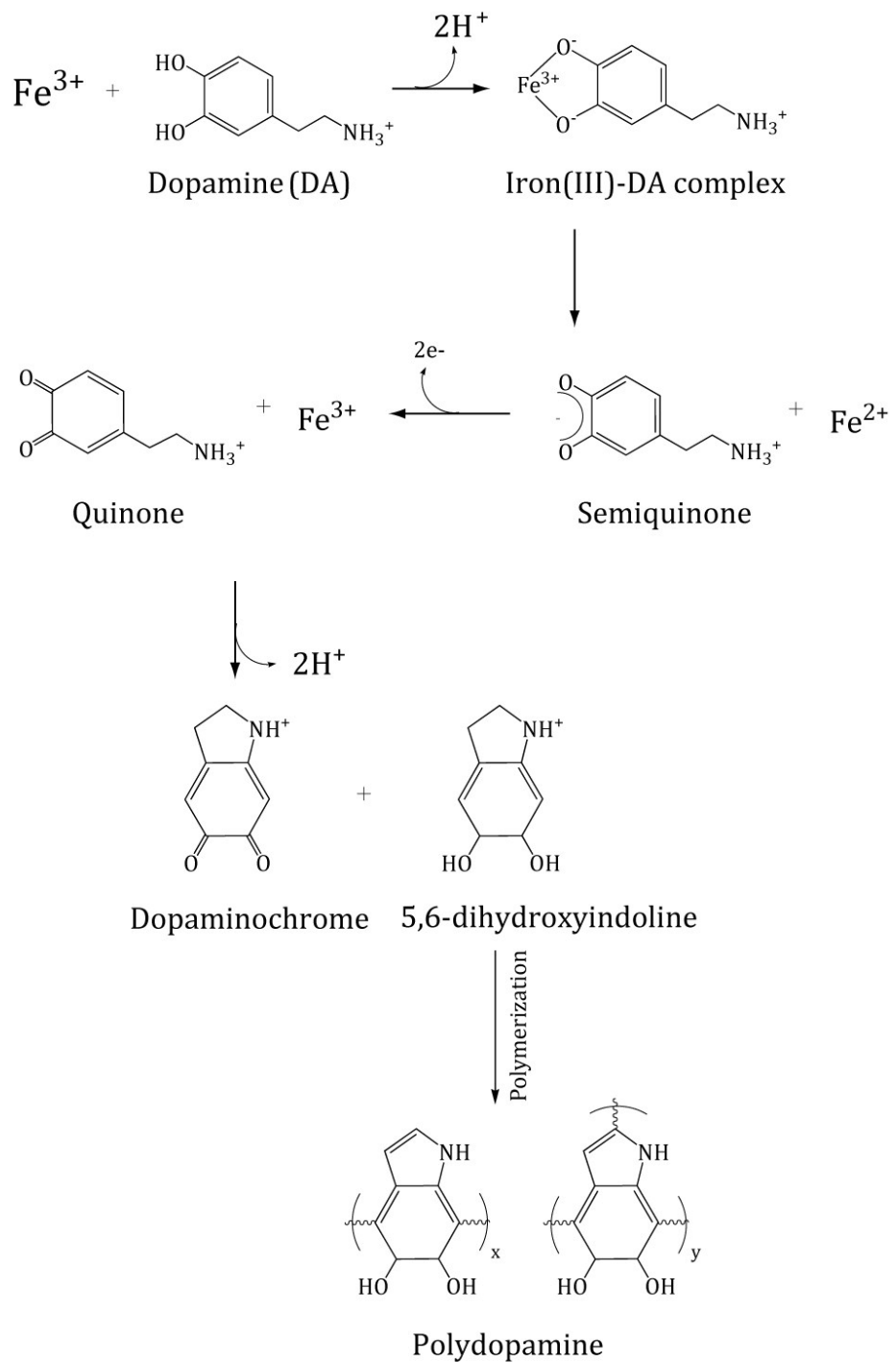
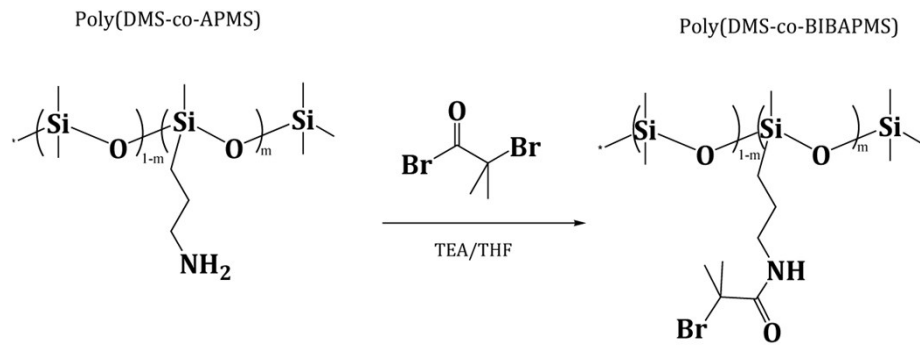


Figure S1. SEM microphotographs of the cross section of a) PDMS initiator layer and b) the ultra-thin CAP film of PEGDMA9 with 15 wt% FeDA₉ NPs incorporated. The scale bar represents 0.5 μm .



Scheme S1. Overall route of formation of iron dopamine nanoparticles.



Scheme S2. Synthesis of the PDMS macroinitiator poly(DMS-co-BIBAPMS).

Table S3. Chemical composition of 15 wt% FeDA nanoparticles preparation in CAP solution.

Sample	Molar ratio (DA/Fe ³⁺)	Fe ³⁺ [mM]	DA [mM]
FeDA ₃	3	2.64	7.91
FeDA ₆	6	1.48	8.90
FeDA ₉	9	1.04	9.28
FeDA ₁₂	12	0.789	9.49

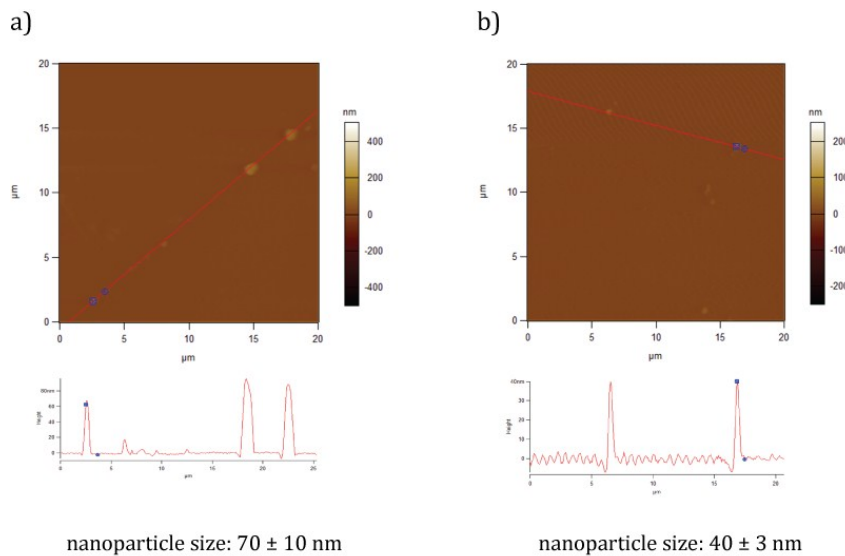


Figure S2. The height mode images and the z-profile for a) FeDA₃ and b) FeDA₉ nanoparticles prepared onto a silicon wafer.

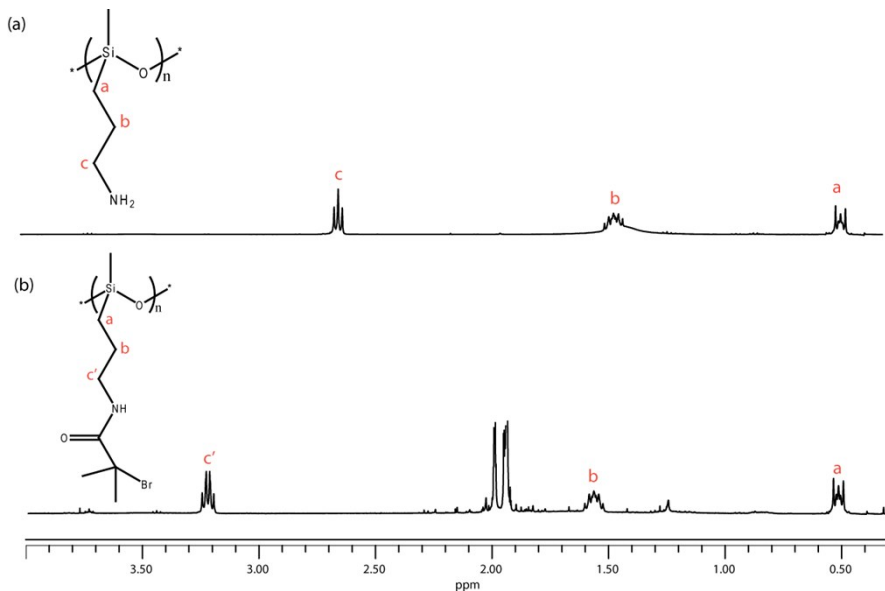


Figure S3. ¹H NMR spectra of (a) 7 % aminopropylmethyl siloxane(dimethylsiloxane) copolymer (P(DMS-*co*-APMS)) and (b) P(DMS-*co*-BIBAPMS).

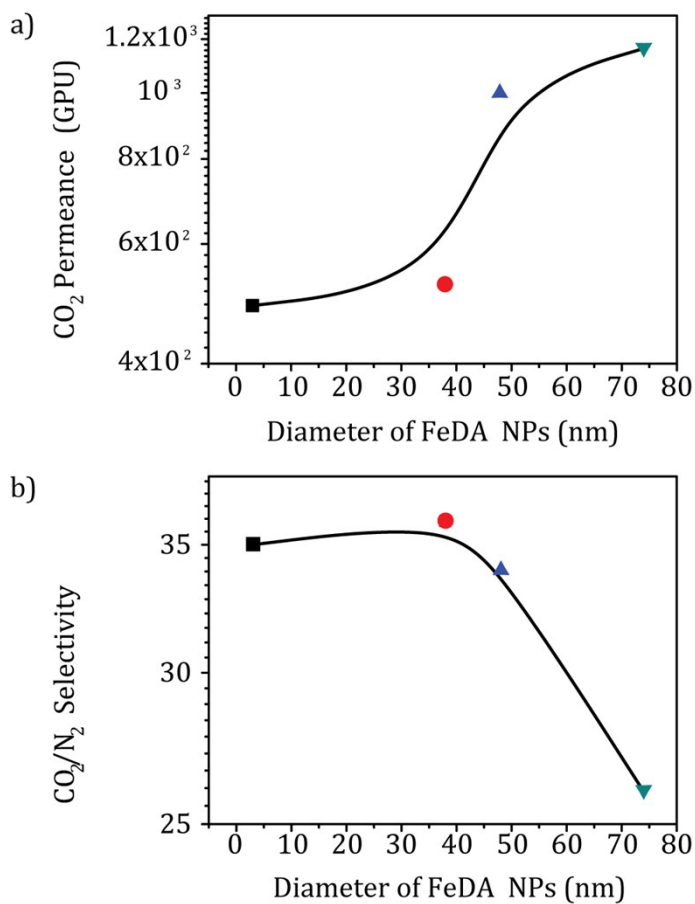
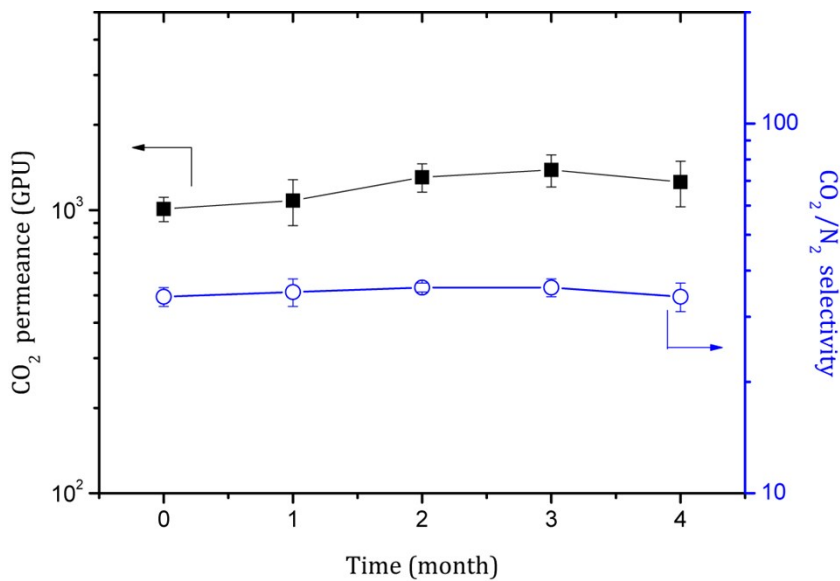


Figure S4. CO₂ permeance (a, solid symbol) and CO₂/N₂ selectivity (b, open symbol) of 15 wt% FeDA₃ (\blacktriangledown), FeDA₆ (\blacktriangle), FeDA₉ (\bullet) and FeDA₁₂ (\blacksquare) incorporated PEGDMA9 UTC-MMMs with different nanoparticle size. Polymerization time: 4 h.

Figure S5. Long-term stability of 15 wt% FeDA₆ NPs incorporated UTFC-MMM.^a

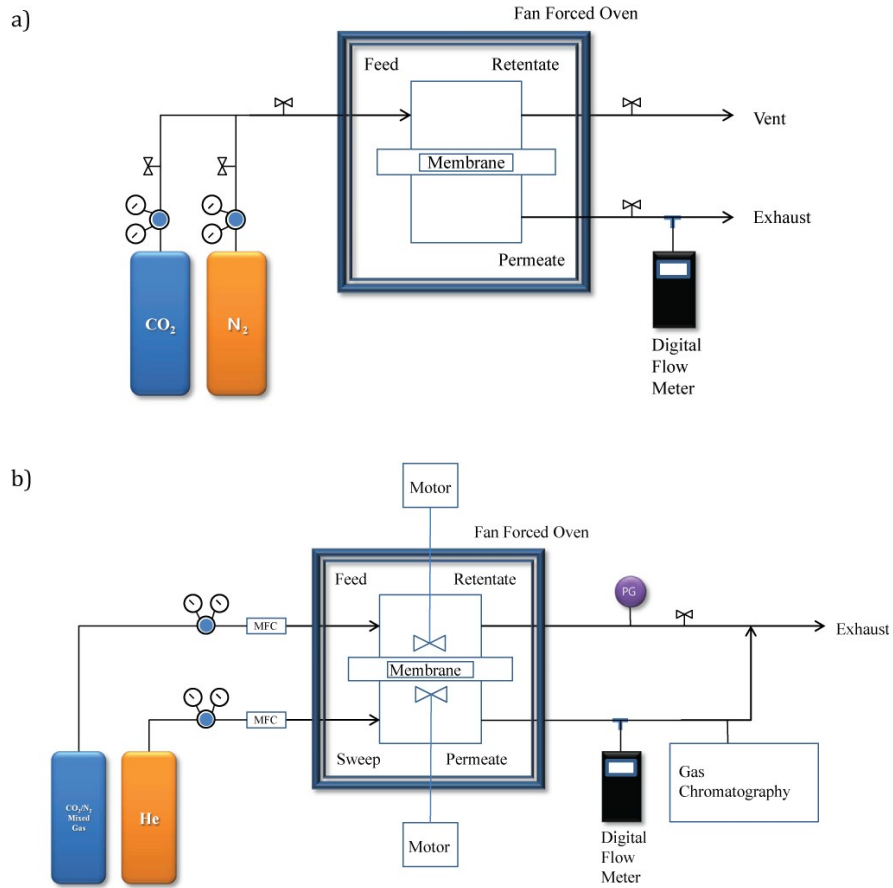


^a The UTFC-MMM was stored under atmospheric conditions (air, 1 atm, 25 °C) and the experiment was conducted at intervals of one month, for 4 months.

Table S4. The chemical stability of 15wt% FeDA₆ NPs incorporated UTFC-MMM reported in this study^a in comparison with that of other UTFC membranes reported in our previous study^{b,c}.

	Original		After treatment	
	P _{CO₂} (GPU)	α (CO ₂ /N ₂)	P _{CO₂} (GPU)	α (CO ₂ /N ₂)
15wt% FeDA ₆ /PEGDMA9 ^a	1010	34	1212	33
PEG UTFC membrane ^b	1140	22	1200	20
Pebax/PEG-50% ^c	899	24	950	14

^a Composite membranes were exposed to a 30.6 mM H₂SO₄ solution for 12 hours, *dried in vacuo* overnight and tested for their gas separation performance. ^b PEG-based ultra-thin film composite membrane, ref[25]. ^c Blended composite membranes (Pebax2533 with 50% wt. PEG-based additives) reported in our previous study^[37].



Scheme S3. Gas permeation testing set-up for a) single gas and b) mixed gas.

Table S5. Summary of CO₂ separation properties for the FeDA NPs incorporated UTFC-MMMs , tested at 35 °C and 350 kPa upstream pressure via single gas test rig. Some data are not presented due to the defects within the selective layer, produced by incorporation of large nanoparticles into a thin selective layer.

Sample	Overall layer		Selective layer	
	FeDAX/PEGDMA9 [wt%]	J_{CO_2} [STP, GPU]	$\alpha(CO_2/N_2)$	J_{CO_2} [STP, GPU]
FeDA ₃				
7.7	820	31	1370	42
15	1165	26	2555	42
30	2560	10	-	-
FeDA ₆				
7.7	870	35	1410	46
15	1010	34	1760	48
30	2255	10	-	-
FeDA ₉				
7.7	375	30	480	33
15	525	36	725	42
30	790	38	1220	51
FeDA ₁₂				
7.7	245	31	300	33
15	490	35	660	42
30	825	44	1315	61

Table S6. Feed gas flow rate dependence of gas separation properties for 15 wt% FeDA₆ NPs incorporated UTFC-MMMs under 30% CO₂/ 70% N₂ mixed gas conditions. Feed stirring rate: 800 rpm, Permeate stirring rate: 400 rpm, sweep flow rate: 250 ml min⁻¹, feed pressure: 1 bar gauge and operation temperature: 35 °C.

Feed flow rate [L min ⁻¹]	P _{CO₂} [GPU]	P _{N₂} [GPU]	α (CO ₂ /N ₂)	Retentate	
				CO ₂ [mol%]	N ₂ [mol%]
0.6	910	83	11	27.66	72.34
1.35	1021	83	12	28.17	71.83
3.1	1082	78	14	29.07	70.93
4.9	1120	83	14	30.31	69.69
6.3	1092	80	14	30.30	69.70

Table S7. Sweep gas flow rate dependence of gas separation properties for 15 wt% FeDA₆ NPs incorporated UTFC-MMMs under 30% CO₂/ 70% N₂ mixed gas conditions. Feed stirring rate: 800 rpm, Permeate stirring rate: 400 rpm, feed flow rate: 4.9 L min⁻¹, feed pressure: 1 bar gauge and operation temperature: 35 °C.

Sweep flow rate [L min ⁻¹]	P _{CO₂} [GPU]	P _{N₂} [GPU]	α (CO ₂ /N ₂)	Retentate	
				CO ₂ [mol%]	N ₂ [mol%]
0.1	1230	95	13	30.42	69.58
0.25	1120	83	14	30.31	69.69
0.89	1110	85	13	29.85	70.15

Table S8. Feed stirring rate dependence of gas separation properties for 15 wt% FeDA₆ NPs incorporated UTFC-MMMs under 30% CO₂/ 70% N₂ mixed gas conditions. Permeate stirring rate: 400 rpm, feed flow rate: 4.9 L min⁻¹, sweep flow rate: 100 ml min⁻¹, feed pressure: 1 bar gauge and operation temperature: 35 °C.

Stirring rate [rpm]	P _{CO₂} [GPU]	P _{N₂} [GPU]	α (CO ₂ /N ₂)
0	943	73	13
200	939	73	13
400	1137	87	13
800	1188	90	13
1300	1235	91	14
1650	1254	93	14
2000	1255	90	14

Table S9. Permeate stirring rate dependence of gas separation properties for 15 wt% FeDA₆ NPs incorporated UTFC-MMMs under 30% CO₂/ 70% N₂ mixed gas conditions. Feed stirring rate: 1650 rpm, feed flow rate: 4.9 L min⁻¹, sweep flow rate: 100 ml min⁻¹, feed pressure: 1 bar gauge and operation temperature: 35 °C.

Stirring rate [rpm]	P _{CO₂} [GPU]	P _{N₂} [GPU]	α (CO ₂ /N ₂)
0	1263	84	15
200	1176	84	14
400	1153	82	14

In Table S6, concentration polarization was detected by GC measurement when feed flow rates were low (0.6 – 3.1 L min⁻¹), followed by enhanced CO₂ permeance at high flow rates (over 4.9 L min⁻¹). In addition, the concentration polarization effect was eliminated as increased stirring rate

on feed stream in Table S8. However, there was a decrease in CO₂ permeance as the sweep flow rate increased. This probably reflects an increasing backpressure on the permeate side, which was not accounted for in calculating the permeance. For the same reason, it can be seen that the CO₂ permeance drops across a range of high stirring rates on the permeate stream in Table S9. Consequently, the optimized experimental conditions showing minimized concentration polarization under the designed mixed gas permeation experiment were feed gas flow rate of 4.9 L min⁻¹, sweep gas flow rate of 0.1 L min⁻¹, feed stirring rate of 1650 rpm and permeate stirring rate of 0 rpm.

Table S10. The effect of SO₂ on the UTFC membrane performance.^a

	before aging		after aging	
	P CO ₂ [GPU]	α (CO ₂ /N ₂)	P CO ₂ [GPU]	α (CO ₂ /N ₂)
PEGDMA9 ^b	1000	21	953	24
15 wt% FeDA ₆ /PEGDMA9	1010	34	995	34

^a Composite membranes were exposed to 500 ppm SO₂ at 1 bar (absolute pressure) for 24 hrs and tested for their gas separation performance. ^b PEG-based ultra-thin film composite membrane.^[38]

1. Resistance Model

Permeation of a gas component *i* across a polymeric membrane can be expressed by Equation S1.

$$Q_i = P_i A \Delta p_i / l \quad (\text{Equation S1})$$

where Q_i is the gas permeate rate of component *i* (cm³ (STP) s⁻¹), P_i is the intrinsic permeability of the membrane to component *i* (cm³ (STP) cm cm⁻² s⁻¹ cmHg⁻¹), A is the membrane surface area (cm²), Δp_i is the partial pressure difference of component *i* across the membrane (cmHg) and l is the membrane thickness (cm).

The relationship describing the permeation of gas component *i* over a polymeric membrane is mathematically comparable to current flow through a resistor according to Ohm's law.

$$I = E / R \quad (\text{Equation S2})$$

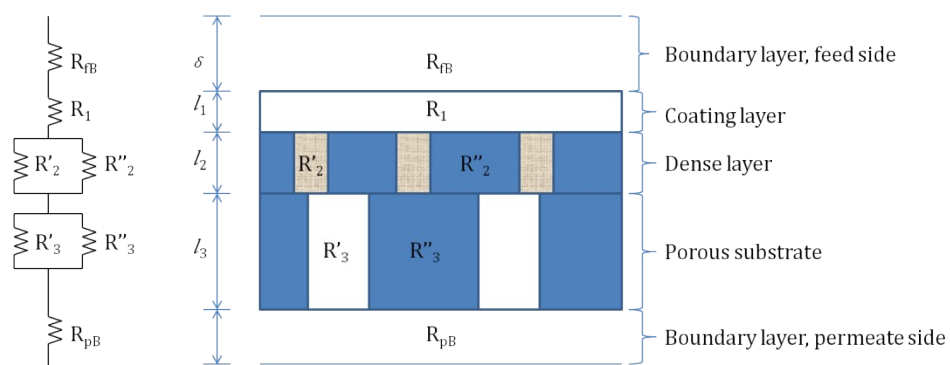
The current I can be compared to the permeation of gas component through the polymeric membrane (Q_i). The driving force of the current flow (E) can be identical to the partial pressure difference (Δp_i) of component i . Then, we can assume that a resistance to permeate component i across the membrane (R_i) is equal to the electrical resistance.

$$R_i = l / P_i A \quad (\text{Equation S3})$$

Thus, the reversely proportional relationship of gas permeation rate to the gas permeation resistance over the polymeric membrane can be expressed by Equation S4 combining Equation S1 and Equation S3. [39]

$$Q_i = \Delta p_i / R_i \quad (\text{Equation S4})$$

In the thin film composite membranes, the relationship is more complicated to explain the resistance resulting from each layer. A possible configuration of thin film composite membrane is shown in Scheme S4.



Scheme S4. A schematic diagram demonstrating the structure of thin film composite membrane with an electrical circuit analog.

The composite membrane consists of three different layers: selective coating layer, highly gas permeable gutter layer and porous substrate. In addition, it is expected that the boundary layer in

the feed and permeation side of membrane can add a resistance through concentration polarization (R_{pB} and R_{fB}). Although the concentration polarization can be ignored in case of the polymeric membrane showing low permeate flux, the concentration polarization effect is more obvious for high flux membrane (over 100 GPU, 1 GPU = 10^{-6} cm³ (STP) cm⁻² s⁻¹ cmHg⁻¹).^[40-41] The total resistance to permeate component i across the thin film composite membrane R_t is the sum of the resistance R_m of the thin film composite membrane, the resistance R_{fB} of boundary layer in feed side and the resistance R_{pB} of boundary layer in permeate side (Equation S5).^[42]

$$R_t = R_m + R_{fB} + R_{pB} \quad (\text{Equation S5})$$

The resistance of boundary layers (R_{fB} and R_{pB}) resulted from concentration polarization can be minimized by increasing feed gas velocity and continuously sweeping the permeate with carrier gas.^[41] Thus, the total resistance is mainly produced by the resistance R_m of the thin film composite membrane, which is a function of the resistance to transport component i in each layer: the resistance of the selective coating layer R_1 , the resistance of the pores or defects in the gutter layer R_2' , the resistance of the dense parts of the gutter layer R_2'' , the resistance of the pores in the porous substrate R_3' and the resistance of the dense parts of the porous substrate R_3'' , expressed in Equation S6.

$$R_t = R_m = R_1 + \frac{R_2' R_2''}{R_2' + R_2''} + \frac{R_3' R_3''}{R_3' + R_3''} \quad (\text{Equation S6})$$

The resistance resulting from the porous substrate is a function of the tortuosity and porosity (R_3'/R_3''). This resistance can be significant if pores fill with the gutter layer material during fabrication. If the penetration of the gutter layer into the pores of porous substrates is avoided (penetrated only 0.1 or 0.01 % of depth)^[39], the resistance of the pores in the porous substrate R_3' can be negligible.^[43] Then,

$$R_t = R_m = R_1 + \frac{R_2' R_2''}{R_2' + R_2''} \quad (\text{Equation S7})$$

Based on Equation S3, these each resistance unit can be expressed by

$$R_1 = \frac{l_1}{P_1 A} \quad (\text{Equation S 8})$$

$$R_2' = \frac{l_2}{P_1 A \varepsilon} \quad (\text{Equation S9})$$

$$R_2'' = \frac{l_2}{P_2 A (1 - \varepsilon)} \quad (\text{Equation S10})$$

and combined Equation S8, S9 and S10 into Equation S7, therefore

$$R_t = \frac{l_1}{P_1 A} + \frac{l_2}{P_1 A \varepsilon + P_2 A (1 - \varepsilon)} \quad (\text{Equation S11})$$

where ε is the defects of the gutter layer ($\varepsilon \ll 1$) and P_1 and P_2 are the intrinsic gas permeability of the selective coating layer and the gutter layer, respectively. As long as ε is near to zero (a defect-free gutter layer), the total resistance of thin film composite membrane R_t can be expressed by Equation S12 and S13.

$$R_t = \frac{l_1}{P_1 A} + \frac{l_2}{P_2 A} \quad (\text{Equation S12})$$

$$R_t = R_1 + R_2 \quad (\text{Equation S13})$$

In addition, the total resistance can be represented by Equation S14.

$$R_T = \Delta p \frac{A_m}{N_{VT}} \quad (\text{Equation S 14})$$

Where Δp is the pressure difference over the membrane, A_m is the gas permeation area of the membrane and N_{VT} is the total flux on the permeate side. Combining Equation S13 and S14, the

flux of the selective layer (N_{SL}) can be obtained from the measurements of the total flux and the flux through the gutter layer (N_G), expressed in Equation S15.

$$N_{SL} = \frac{N_{VT} N_G}{N_G - N_{VT}} \quad (\text{Equation S15})$$

As the resistance of the selective layer is directly related to the thickness (l) and permeability (P), the gas permeance over the selective layer (P_{SL}) can be calculated from Equation S16.

$$P_{SL} = \frac{N_{SL} l}{A_m \Delta P} \quad (\text{Equation S16})$$

REFERENCES

- [1] W. Yave, A. Car, S. S. Funari, S. P. Nunes and K.-V. Peinemann, *Macromolecules* **2009**, *43*, 326-333.
- [2] J. Peter and K.-V. Peinemann, *Journal of Membrane Science* **2009**, *340*, 62-72.
- [3] W. F. Yong, F. Y. Li, Y. C. Xiao, T. S. Chung and Y. W. Tong, *Journal of Membrane Science* **2013**, *443*, 156-169.
- [4] G. Kapantaidakis and G. Koops, *Journal of Membrane Science* **2002**, *204*, 153-171.
- [5] T. Visser, G. Koops and M. Wessling, *Journal of Membrane Science* **2005**, *252*, 265-277.
- [6] T. Visser, N. Masetto and M. Wessling, *Journal of Membrane Science* **2007**, *306*, 16-28.
- [7] C. A. Scholes, G. Q. Chen, G. W. Stevens and S. E. Kentish, *Journal of Membrane Science* **2010**, *346*, 208-214.
- [8] X. Ren, J. Ren, H. Li, S. Feng and M. Deng, *International Journal of Greenhouse Gas Control* **2012**, *8*, 111-120.
- [9] A. Car, C. Stropnik, W. Yave and K.-V. Peinemann, *Separation and Purification Technology* **2008**, *62*, 110-117.
- [10] H. Z. Chen, Z. Thong, P. Li and T.-S. Chung, *International Journal of Hydrogen Energy* **2014**, *39*, 5043-5053.
- [11] L. Liu, A. Chakma and X. Feng, *Chemical Engineering Journal* **2004**, *105*, 43-51.
- [12] J. Zhou, M.-M. Tran, A. T. Haldeman, J. Jin, E. H. Wagener and S. M. Husson, *Journal of Membrane Science* **2014**, *450*, 478-486.
- [13] H. Z. Chen, Y. C. Xiao and T.-S. Chung, *Journal of Membrane Science* **2011**, *381*, 211-220.
- [14] C. M. Spadaccini, E. V. Mukerjee, S. A. Letts, A. Maiti and K. C. O'Brien, *Energy Procedia* **2011**, *4*, 731-736.
- [15] H. Suzuki, K. Tanaka, H. Kita, K. Okamoto, H. Hoshino, T. Yoshinaga and Y. Kusuki, *Journal of Membrane Science* **1998**, *146*, 31-37.
- [16] L. Hao, J. Zuo and T. S. Chung, *AIChE Journal* **2014**, *60*, 3848-3858.
- [17] R. P. Lively, M. E. Dose, L. Xu, J. T. Vaughn, J. Johnson, J. A. Thompson, K. Zhang, M. E. Lydon, J.-S. Lee and L. Liu, *Journal of Membrane Science* **2012**, *423*, 302-313.

- [18] S. Kulprathipanja, *Annals of the New York Academy of Sciences* **2003**, *984*, 361-369.
- [19] R. Xing and W. Ho, *Journal of Membrane Science* **2011**, *367*, 91-102.
- [20] C. Hibshman, C. Cornelius and E. Marand, *Journal of Membrane Science* **2003**, *211*, 25-40.
- [21] S. N. Wijenayake, N. P. Panapitiya, S. H. Versteeg, C. N. Nguyen, S. Goel, K. J. Balkus Jr, I. H. Musselman and J. P. Ferraris, *Industrial & Engineering Chemistry Research* **2013**, *52*, 6991-7001.
- [22] M. Sforca, I. Yoshida and S. Nunes, *Journal of Membrane Science* **1999**, *159*, 197-207.
- [23] Y. C. Hudiono, T. K. Carlisle, A. L. LaFrate, D. L. Gin and R. D. Noble, *Journal of Membrane Science* **2011**, *370*, 141-148.
- [24] Y. Dai, J. Johnson, O. Karvan, D. S. Sholl and W. Koros, *Journal of Membrane Science* **2012**, *401*, 76-82.
- [25] T. Li, Y. Pan, K.-V. Peinemann and Z. Lai, *Journal of Membrane Science* **2013**, *425*, 235-242.
- [26] R. S. Murali, S. Sridhar, T. Sankarshana and Y. Ravikumar, *Industrial & Engineering Chemistry Research* **2010**, *49*, 6530-6538.
- [27] Y. Li and T.-S. Chung, *international journal of hydrogen energy* **2010**, *35*, 10560-10568.
- [28] F. Moghadam, M. Omidkhah, E. Vasheghani-Farahani, M. Pedram and F. Dorost, *Separation and Purification Technology* **2011**, *77*, 128-136.
- [29] E. V. Perez, K. J. Balkus, J. P. Ferraris and I. H. Musselman, *Journal of Membrane Science* **2009**, *328*, 165-173.
- [30] D. Q. Vu, W. J. Koros and S. J. Miller, *Journal of Membrane Science* **2003**, *211*, 311-334.
- [31] B. D. Reid, F. A. Ruiz-Trevino, I. H. Musselman, K. J. Balkus and J. P. Ferraris, *Chemistry of materials* **2001**, *13*, 2366-2373.
- [32] M. Junaidi, C. Leo, A. Ahmad, S. Kamal and T. Chew, *Fuel Processing Technology* **2014**, *118*, 125-132.
- [33] M. G. Süer, N. Baç and L. Yilmaz, *Journal of Membrane Science* **1994**, *91*, 77-86.
- [34] R. Adams, C. Carson, J. Ward, R. Tannenbaum and W. Koros, *Microporous and Mesoporous Materials* **2010**, *131*, 13-20.
- [35] J. Ahmad and M.-B. Hägg, *Journal of Membrane Science* **2013**, *427*, 73-84.
- [36] H. Cong, M. Radosz, B. F. Towler and Y. Shen, *Separation and Purification Technology* **2007**, *55*, 281-291.
- [37] Q. Fu, A. Halim, J. Kim, J. M. Scofield, P. A. Gurr, S. E. Kentish and G. G. Qiao, *Journal of Materials Chemistry A* **2013**, *1*, 13769-13778.
- [38] Q. Fu, J. Kim, P. A. Gurr, J. M. Scofield, S. E. Kentish and G. G. Qiao, *Energy & Environmental Science* **2015**.
- [39] J. M. Henis and M. K. Tripodi, *Journal of membrane science* **1981**, *8*, 233-246.
- [40] O. Lüdtke, R.-D. Behling and K. Ohlrogge, *Journal of membrane science* **1998**, *146*, 145-157.
- [41] G. He, Y. Mi, P. L. Yue and G. Chen, *Journal of membrane science* **1999**, *153*, 243-258.
- [42] F. Peng, J. Liu and J. Li, *Journal of membrane science* **2003**, *222*, 225-234.
- [43] I. Vankelecom, B. Moermans, G. Verschueren and P. Jacobs, *Journal of membrane science* **1999**, *158*, 289-297.